A Novel High-Affinity Inhibitor for Inward-Rectifier K^+ Channels†

Weili Jin and Zhe Lu*

Department of Physiology, University of Pennsylvania, 3700 Hamilton Walk, Philadelphia, Pennsylvania 19104

Received May 19, 1998; Revised Manuscript Received July 2, 1998

ABSTRACT: Inward-rectifier K^+ channels are a group of highly specialized K^+ channels that accomplish a variety of important biological tasks. Inward-rectifier K^+ channels differ from voltage-activated K^+ channels not only functionally but also structurally. Each of the four subunits of the inward-rectifier K^+ channels has only two instead of six transmembrane segments compared to the voltage-activated K^+ channels. Thus far, there are no high-affinity ligands that directly target any inward-rectifier K^+ channel. In the present study, we identified, purified, and synthesized a protein inhibitor of the inward-rectifier K^+ channels. The inhibitor, called tertiapin, blocks a G-protein-gated channel (GIRK1/4) and the ROMK1 channel with nanomolar affinities, but a closely related channel, IRK1, is insensitive to tertiapin. Mutagenesis studies show that teritapin inhibits the channel by binding to the external end of the ion conduction pore.

Inward-rectifier K^+ channels function like K^+-selective diodes in the cell membrane (*1, 2*). They pass much larger inward than outward K^+ current under symmetric ionic conditions. This unusual property is commonly referred to as inward rectification, which results from voltage-dependent blockade by intracellular cations such as Mg^{2+} and polyamines (*3*−*8*). Under physiological conditions, inward rectification manifests itself as a progressive reduction of the outward current, which allows the channel to control and regulate the resting membrane potential without impeding the generation of action potentials. Through regulation of the resting membrane potential, inward-rectifier K^+ channels accomplish many important and diversified biological tasks. For example, the G-protein-gated K^+ channels control the heart rate and modulate neurotransmission; the ATP-sensitive K^+ channel couples blood glucose level to insulin secretion; the ROMK1 channel mediates water and electrolyte excretion in the kidney (*2, 9*−*14*). The activities of most, if not all, inward-rectifier K^+ channels are regulated by intracellular signaling pathways such as G-proteins, inositol phosphates, and protein kinases (*2, 15*−*21*).

Inward-rectifier K^+ channels differ from voltage-activated K^+ channels not only in function but also in structure. Each of the four subunits of the inward-rectifier K^+ channels has only two transmembrane segments rather than six found in voltage-activated K^+ channels (*9*−*14*). The amino acid sequences between the two channel types are minimally conserved except for the signature sequence (T-X-X-T-X-G-Y/F-G) that forms the K^+-selective filter (*22*−*24*). Although most of the inward-rectifier K^+ channels are formed by four identical subunits, some channels are formed by nonidentical subunits. A good example for the latter is the G-protein-gated inward-rectifier K^+ channel (GIRK1/4) in the heart, which is formed by two different types of subunits, GIRK1(GSK) and GIRK4(CIR) (*11*−*13*). In some cases, the channels are complexed with other proteins. For example, the ATP-sensitive K^+ channel is a complex of an inward-rectifier K^+ channel (K_{ir} 6.2) and sulfonylurea receptor (*14*).

Thus far, the pharmacology of inward-rectifier K^+ channels is poorly developed. There are no high-affinity ligands that directly target any inward-rectifier K^+ channels. Out of a number of scorpion toxins that target K^+ channels, only Lq2 blocks the ROMK1 inward-rectifier K^+ channel, but the affinity is rather low ($K_d = 0.4\ \mu M$) (*25*; for Lq2, also see *26*, *27*). Because high-affinity inhibitors prove to be very valuable tools for the studying of ion channels, we decided to search for high-affinity inhibitors against inward-rectifier K^+ channels.

MATERIALS AND METHODS

Channel Expression. Oocytes harvested from *Xenopus laevis* frogs were digested with collagenase (2 mg/mL) in a solution containing NaCl, 82.5 mM; KCl, 2.5 mM; $MgCl_2$, 1.0 mM; and HEPES, 5.0 mM (pH 7.6), and were agitated on a platform shaker at a rate of 80 rpm for 90 min. The oocytes were then rinsed thoroughly with and stored in a solution containing gentamicin, 50 μg/mL; NaCl, 96 mM; KCl, 2 mM; $CaCl_2$, 1.8 mM; $MgCl_2$, 1 mM; and HEPES, 5 mM (pH 7.6). Defolliculated oocytes were selected at least 2 h after the collagenase digestion. To express channels, the corresponding cRNA was directly injected into oocytes. To express the GIRK1/4 channel, GIRK1 and GIRK4 cRNAs were coinjected with either M2 or M4 receptor cRNA. All injections were carried out at least 16 h after the collagenase treatment. The injected oocytes were stored in a 18 °C incubator.

Channel Recording. All three inward-rectifier K^+ channels, GIRK1/4, ROMK1, and IRK1, were studied using a two-electrode voltage clamp amplifier (Oocyte Clamp OC-

† This work was supported by an NIH grant (GM55560).

* Correspondence should be addressed to this author at the Department of Physiology, University of Pennsylvania, D302A Richard Building, 3700 Hamilton Walk, Philadelphia, PA 19104. Telephone: 215-573-7711. FAX: 215-573-5851. Email: zhelu@mail.med.upenn.edu.

S0006-2960(98)01178-7 CCC: $15.00
Published on Web 08/29/1998

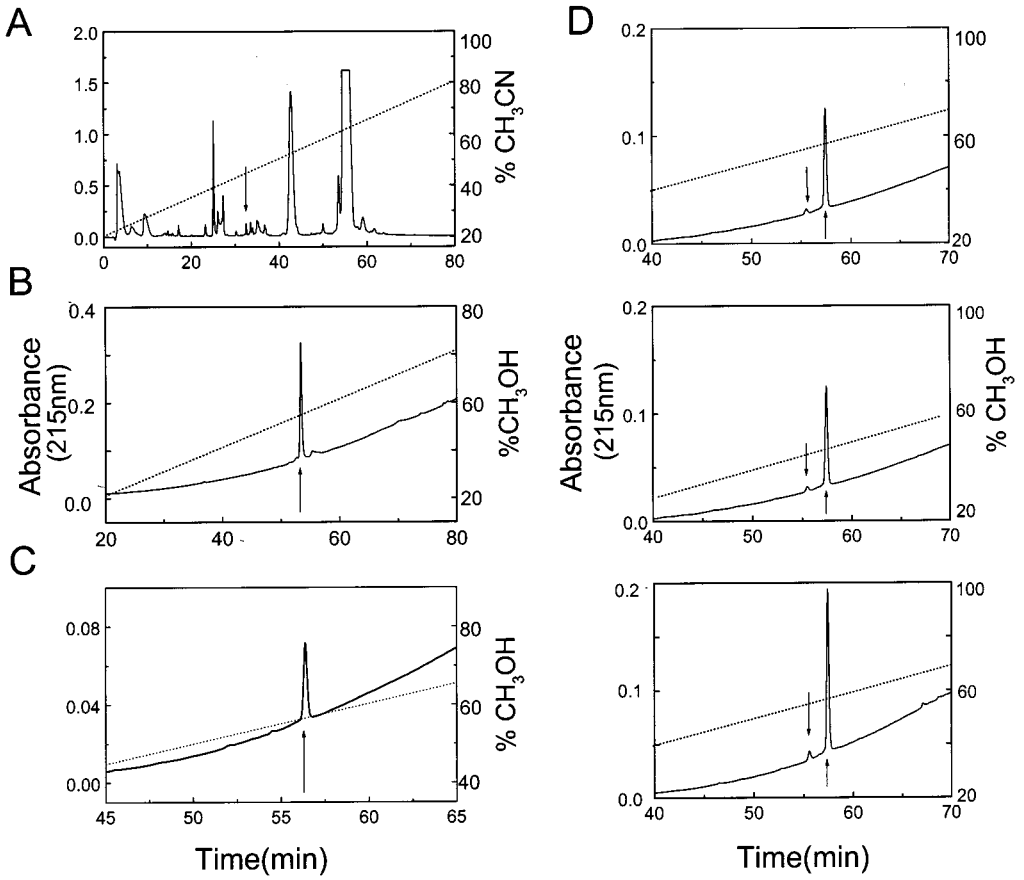

FIGURE 1: Purification of the inhibitor from honey bee venom. (A) A reverse-phase (C18) chromatograph of crude bee venom. A venom suspension of 100 μL (10 mg/1 mL) was injected on the column. Mobile phases A and B were 0.1% TFA (trifluoroacetic acid) in water and 0.09% TFA in acetonitrile, respectively. The venom sample was eluted by increasing the fraction of mobile phase B at a rate of 1% per minute. The fraction containing the active material was indicated by the arrow. (B) A reverse-phase (C18) chromatograph of the active fraction purified as shown in A. Mobile phases A and B were 0.1% TFA in water and 0.07% TFA in methanol, respectively. The sample was eluted by increasing the fraction of mobile phase B at a rate of 1% per minute. The active component was indicated by the arrow. (C) A reverse-phase (C18) chromatograph of the active fraction purified in (B). (D) A comparison of chromatographic behaviors of native and synthetic tertiapin. The samples were native tertiapin (upper), synthetic tertiapin (middle), and the combination of both (lower). For illustration, we used samples containing a small amount of tertiapin whose M13 was oxidized (see *Preparation of the Synthetic Tertiapin* under Materials and Methods). The large absorbance peaks, indicated by upward arrows, corresponded to the nonoxidized form, whereas the much smaller peaks, indicated by downward arrows, corresponded to the oxidized form. The chromatographic method in (C) and (D) was the same as that in panel B but with a different C18 column. In all of the experiments described above, the flow rate of the mobile phase was 1.0 mL/min. (E) Single-letter-coded amino acid sequence of tertiapin, apamin, and MCDP.

725C, Warner Instruments Corp.). The resistance of electrodes filled with 3 M KCl was 0.2−0.4 MΩ. To elicit current through the channel, the membrane potential of oocytes was stepped to −80 mV (100−125 ms) and then to +80 mV (100−125 ms) from the holding potential of 0 mV. Background leak currents were obtained by exposing oocytes to solutions containing tertiapin at concentrations greater than 100-fold of K_d. (Tertiapin did not affect the currents in uninjected oocytes.) The bath solution contained KCl, 100 mM; $CaCl_2$, 0.3 mM; $MgCl_2$, 1.0 mM; and HEPES, 10 mM (pH 7.6). To activate the GIRK1/4 channel, ACh (150 μM) was included in the bath solution. Tertiapin concentration was calculated using an extinction coefficient of 6.1 mM^{-1} cm^{-1} at 280 nm wavelength. All toxin-containing solutions were freshly made by diluting stock solutions. Unless specified otherwise, tertiapin used in all experiments were made synthetically (see below). All other toxins were either recombinant toxins or purchased from Alomone Labs (Jerusalem, Israel).

Molecular Biology. The GIRK1 and GIRK4(CIR) cDNAs were cloned into pBluescript (SK-) plasmid (Stratagene)-(*11, 13*). The ROMK1 and IRK1 cDNAs were cloned into pSPORT (Gibco-BRL) and pcDNA1/AMP (Invitrogen) plasmids (*9, 10*). The M2 and M4 receptor cDNAs were cloned into pGEM3 (Promega) plasmid. A mutation was introduced into the ROMK1 cDNA to create an *Nde*I site without altering the amino acid sequence. Mutations in the ROMK1 cDNA were produced using the polymerase chain reaction (PCR) primed with a mutagenic oligonucleotide. A sequenced 240 base pair fragment containing the mutation (between *Nde*I and *Bgl*II) was subcloned into a wild-type recipient version of the ROMK1 cDNA. The GIRK1,

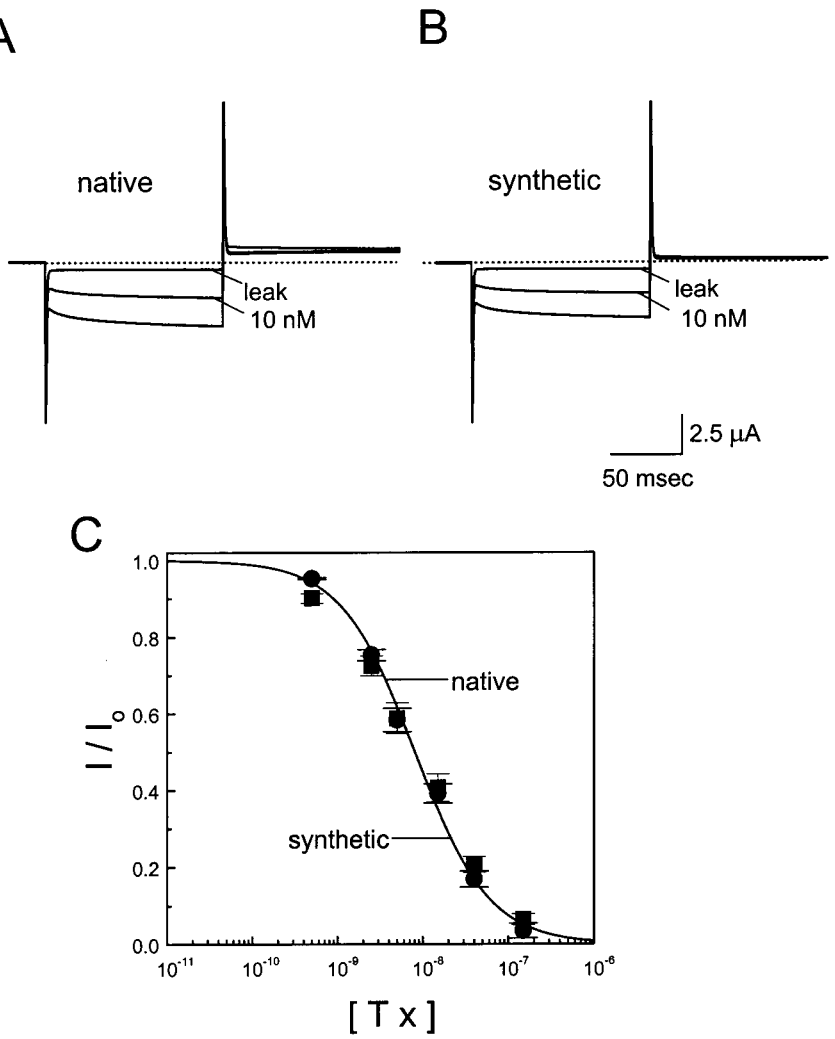

FIGURE 2: Comparison of inhibitory activities of native and synthetic tertiapin. (A and B) Currents through the GIRK1/4 channel were elicited by stepping the membrane potential from the holding potential (0 mV) to −80 mV (125 ms) and then to +80 mV (125 ms). The currents were recorded in the presence of 10 nM of native (A) and synthetic (B) tertiapin. Background leak currents were recorded in the presence of >5 μM tertiapin. Higher concentrations of tertiapin did not further reduce the currents. There was 150 μM ACh in the bath solution. The dotted lines identify the zero current level. (C) Fractions of unblocked current (I/I_o) were plotted as a function of concentrations of native (circles) and synthetic (squares) tertiapin. All data were corrected for the background leak current determined using high concentrations of tertiapin. The curves superimposed on the data correspond to the best least-squares fits using the equation $I/I_o = K_i/(K_i + [Tx])$, where [Tx] is toxin concentration. The determined inhibition constants were 8.2 ± 0.8 and 8.6 ± 0.5 nM (mean ± sem; $n = 21-29$) for native and synthetic tertiapin, respectively.

ROMK1, and IRK1 cDNAs were linearized using *Not*I. The GIRK4 cDNA was linearized using *Xho*I. The M2 and M4 receptor cDNAs were linearized using *Hind*III. All cRNAs, except for that of GIRK4, were synthesized using T7 polymerase (Promega). The GIRK4 cRNA was synthesized using T3 polymerase (Promega).

Purification of Tertiapin. Lyophilized venom of honey bee (*Apis mellifera)* was dissolved in water at a concentration of 10 mg/mL. The venom suspension was first fractionated using a reverse-phase HPLC (high-performance liquid chromatograph) column (C18, 0.46 × 25 cm, 5 μm, 80 Å pore size, Beckman). The sample was eluted with a water and acetonitrile gradient. The active fraction was further purified with an additional step of reverse-phase HPLC, in which the sample was eluted with a water and methanol gradient. The mass of the purified material was determined on a VG analytical MALDI-TOF spectrometer.

Amino Acid Analysis and Sequence Determination. The amino acid analysis was done using a 420A derivatizer and a 103A separation system (Applied Biosystems). The extinction coefficient for tertiapin was calculated by determining the amino acid composition of an aliquot of tertiapin of known absorbance. The amino acid sequence of tertiapin was determined using 477A protein sequencer (Applied Biosystem) after derivatization of cysteine residues with 4-vinylpyridine.

Preparation of the Synthetic Tertiapin. Tertiapin was synthesized using a Rainin/Protein Technologies Symphony multipeptide synthesizer. The determined mass of the synthesized peptide, 2460 daltons, is the same as the theoretical one. Tertiapin spontaneously adopted the correct conformation in a solution containing 1 mM DTT and 10 mM Tris (pH 8.0) after DTT became oxidized. Tertiapin in the correct conformation was subsequently purified using reverse-phase HPLC. We should point out that the methionine residue (M13) in tertiapin may become oxidized spontaneously. Oxidation of M13 altered both the chromatographic behavior and the inhibitory activity of tertiapin.

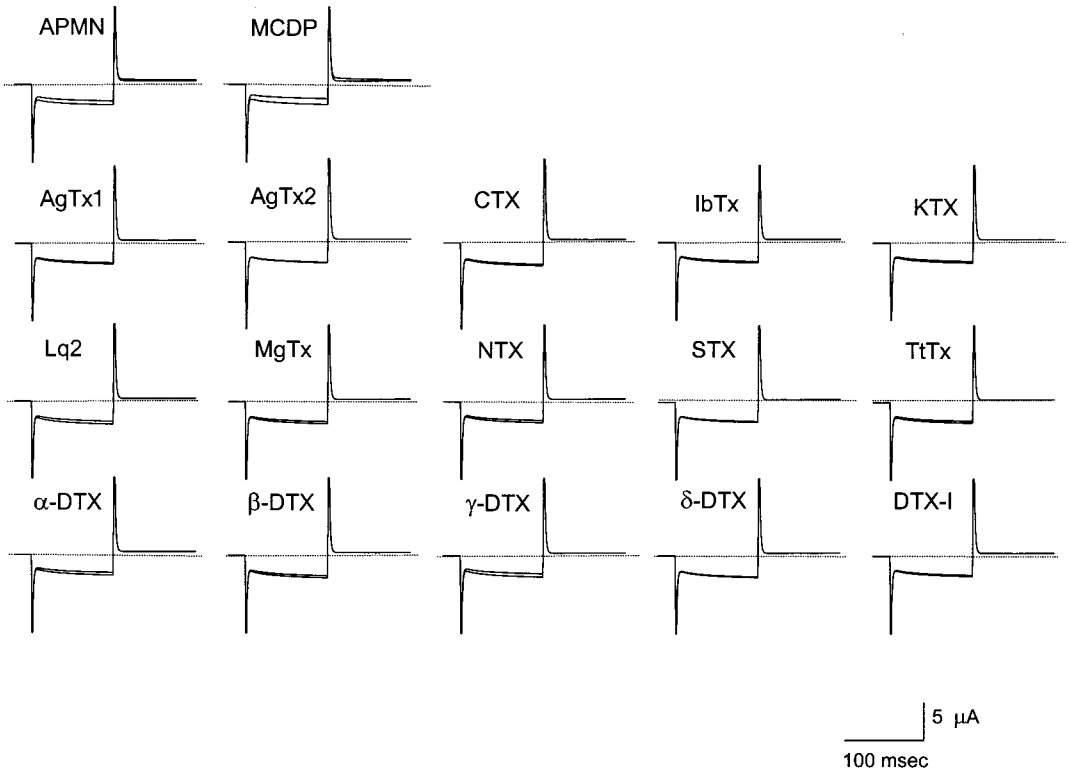

FIGURE 3: Effects of 17 K^+ channel toxins on the GIRK1/4 channel. Currents of the GIRK1/4 channel recorded in the presence of various toxins at 1 μM concentration. There was 150 μM ACh in the bath solution. The dotted lines identify the zero current level. The 17 toxins tested were apamin (APMN), mast cell degranulating peptide (MCDP), agitoxin 1 (AgTx1), agitoxin 2 (AgTx2), charybdotoxin (CTX), iberiotoxin (IbTx), kaliotoxin (KTX), Lq2, margatoxin (MgTx), noxiustoxin (NTX), stichodactyla toxin (STX), tityustoxin (TtTx), α-dendrotoxin (α-DTX), β-dendrotoxin (β-DTX), γ-dendrotoxin (γ-DTX), δ-dendrotoxin (δ-DTX), and dendrotoxin-I (DTX-I).

Table 1: Amino Acid Composition of Tertiapin[a]

	residues/molecule			residues/molecule	
	observed	theoretical		observed	theoretical
Asn, Asp	1.7	2	Pro	1.2	1
Gln, Glu	0.2	0	Try	0.1	0
Ser	0.2	0	Val	0.2	0
Gly	1.3	1	Met	0.7	1
His	1.0	1	I le	1.9	3
Arg	1.0	1	Leu	1.2	1
Thr	0.0	0	Phe	0.2	0
Ala	1.0	1	Lys	4.1	4

[a] The contents of cysteine and tryptophan were not determined.

As shown in Figure 1D, the oxidized form of tertiapin was eluted at a lower percentage of organic phase than the nonoxidized form. The affinity of the oxidized form of tertiapin for the channels was about 20-fold lower than that of the nonoxidized form (data not shown). Therefore, we daily examined our tertiapin samples using HPLC both before and after experiments. We only used tertiapin samples containing less than 1% oxidized tertiapin, which was determined from the areas of absorbance peaks on HPLC.

RESULTS

Purification and Synthesis of an Inhibitor against Inward-Rectifier K^+ Channels. We initially screened venoms from various sources for their activities against the inward-rectifier K^+ channel formed by GIRK1(GSK) and GIRK4(CIR) (*11*−*13*). The channel, GIRK1/4, normally present in cardiac cells and is gated by muscarinic receptors through G-proteins. To study the GIRK1/4 channel, we coexpressed muscarinic receptors along with GIRK1/4 channel in *Xenopus* oocytes. Because oocytes have endogenous G-proteins, the channel can be activated by adding acetylcholine to the bath solution containing 100 mM K^+. The resting membrane potential of oocytes was held at 0 mV. To elicit the current through the channel, membrane voltage was briefly stepped to −80 mV and then to +80 mV. The current was recorded using a two-electrode voltage−clamp amplifier.

We purified the activity in the venom using reverse-phase HPLC. Figure 1A is an HPLC chromatograph of crude honey bee venom. The fraction indicated by an arrow contained the inhibitory activity and was further purified by an additional HPLC step (Figure 1B). The purity of the material was then examined on HPLC (Figure 1C). Amino acid sequencing showed that the purified material consisted of 21 amino acid residues which included 4 cysteines and 5 basic residues (Figure 1E). The predicted and observed masses of the purified material are 2460 and 2458 daltons, respectively. The predicted and observed amino acid compositions of the material are also in a good agreement (Table 1). As we searched protein databases, we found the amino acid sequence of our purified material is the same as that of tertiapin, a previously purified protein from the same venom (*28*, *29*). However, the usage of tertiapin was unknown.

To demonstrate that tertiapin itself is the active component, we compared native tertiapin with synthetic tertiapin (see Materials and Methods). Chromatographic behaviors of the native and the synthetic tertiapin were indistinguishable (Figure 1D). When injected separately, the native and the synthetic tertiapin had an identical retention time on HPLC

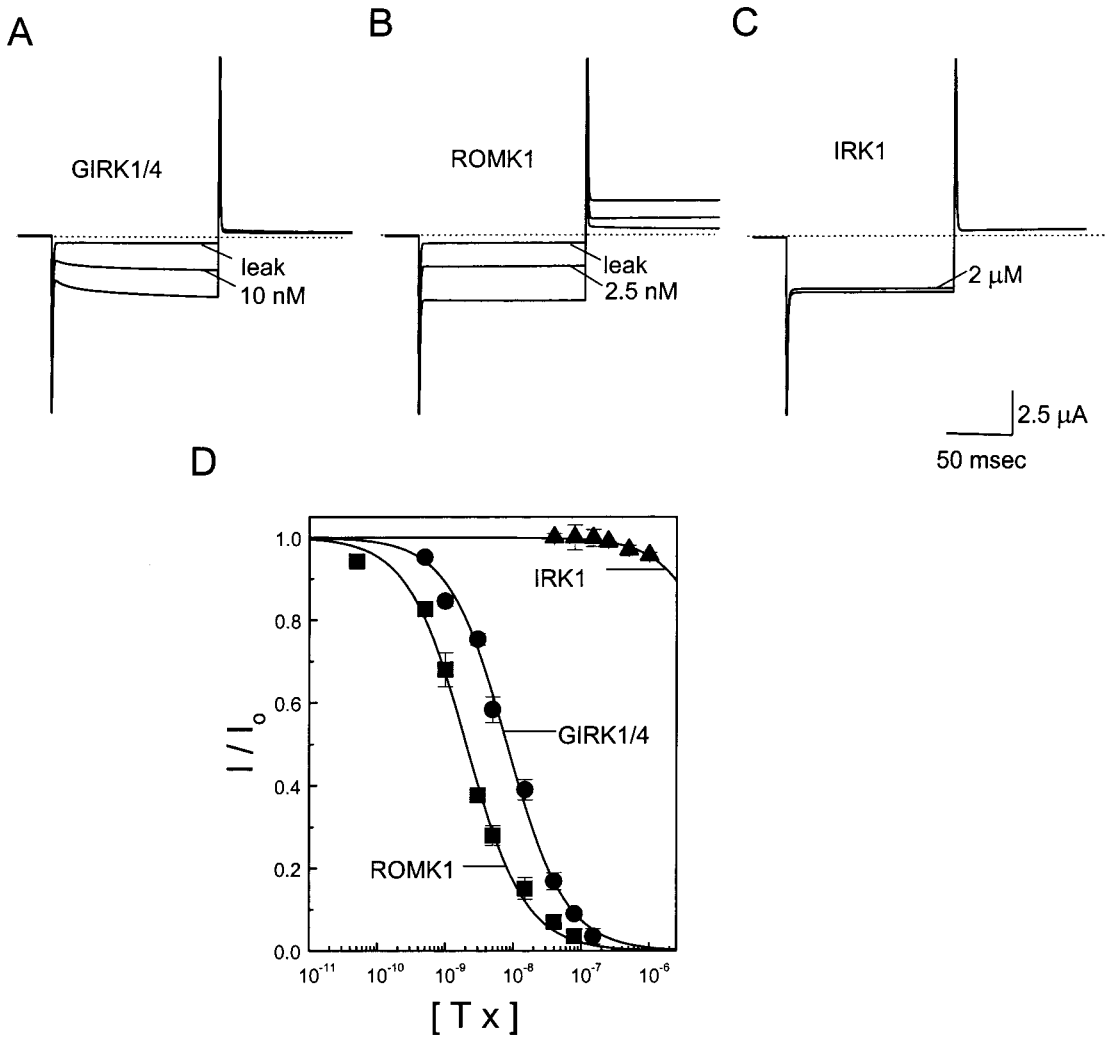

FIGURE 4: Inhibition of three inward-rectifier K^+ channels by tertiapin. (A−C) The current traces of the GIRK1/4 (A), ROMK1 (B), and IRK1 (C) channels recorded in the absence and presence of tertiapin at the concentrations indicated. The dotted lines identify the zero current level. (D) Fractions of unblocked current (I/I_o) for the three channels were plotted as a function of the concentration of tertiapin. Except for the IRK1 channel, all data were corrected for the background leak current, which was determined using high concentrations of tertiapin. The curves superimposed on the data correspond to the best least-squares fits using the equation $I/I_o = K_i/(K_i + [Tx])$, where [Tx] is toxin concentration. The determined inhibition constants were 8.6 ± 0.5 and 2.0 ± 0.1 nM (mean ± sem; $n = 16-29$) for the GIRK1/4 and ROMK1 channels, respectively. The affinity of the IRK1 channel was so low that we could not accurately determine it.

column (upper and middle traces in Figure 1D). When coinjected, the native and synthetic tertiapin comigrated on the column (lower trace in Figure 1D). Functionally, both the native and the synthetic tertiapin had almost identical inhibitory activity. As shown in Figure 2A,B, the native and synthetic tertiapin, each at 10 nM, inhibited the GIRK1/4 current by about 50%. The fraction of unblocked currents in the presence of the native and synthetic tertiapin were plotted as a function of their concentrations (Figure 2C). The curves superimposed on the data represent the best fits of an equation that assumes one tertiapin molecule blocks one channel. The equilibrium dissociation constants determined for the native and synthetic tertiapin were 8.2 and 8.6 nM, respectively.

Specificity of Tertiapin. Two other honey bee toxins, apamin and mast cell degranulating peptide (MCDP), are known to inhibit voltage- and/or Ca^{2+}-activated K^+ channels (*30*, *31*). They share some homology with tertiapin in amino acid sequence (Figure 1E). Therefore, we examined the potential effects of apamin and MCDP on the GIRK1/4 channel. As shown in Figure 3, both apamin and MCDP, at 1 μM concentration, inhibited the channel by only 20−30%. The affinities of the channel ($K_d > 1$ μM) for these two toxins were at least 100-fold lower than that for tertiapin ($K_d = 8$ nM). Furthermore, we examined 15 other toxins derived from various venoms. All of them had little or no effects on the channel at a concentration of 1 μM (Figure 3).

To determine the specificity of tertiapin, we tested it against two other related inward-rectifier K^+ channels, ROMK1 and IRK1 (*9*, *10*). As shown in Figure 4, the ROMK1 channel was also very sensitive to tertiapin. In fact, the ROMK1 channel was even slightly more sensitive to tertiapin than the GIRK1/4 channel. The dissociation constant for tertiapin binding to the ROMK1 channel was 2.0 nM. In contrast, the IRK1 channel was relatively insensitive to tertiapin.

Effects of Channel Mutations on Tertiapin Affinity. To test if tertiapin inhibits the channels by binding to their P-regions, we examined how mutations in the P-region versus other regions affect tertiapin and channel interaction. Since the ROMK1 channel assembles as a homotetramer, we can

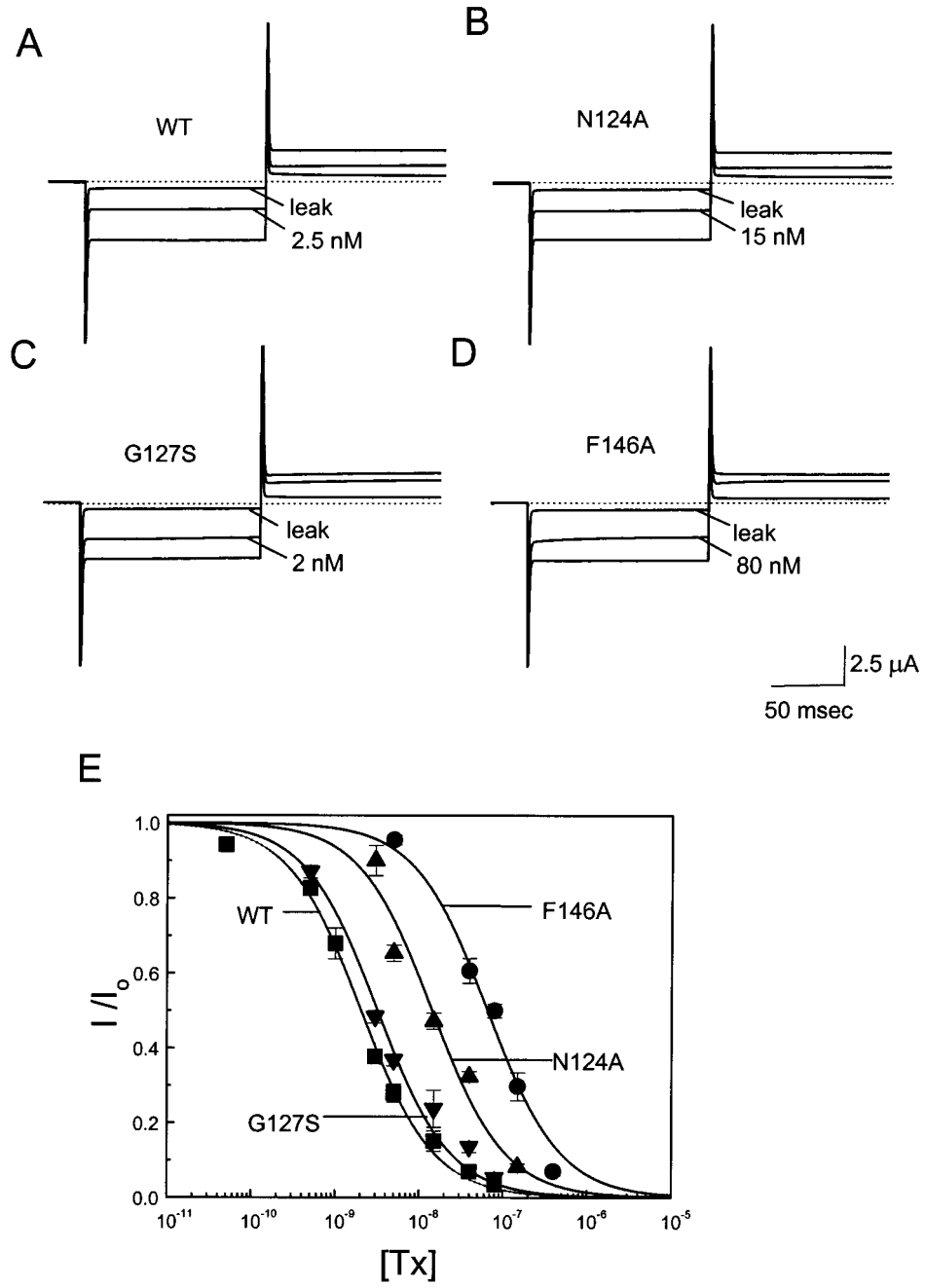

FIGURE 5: Effects of ROMK1 P-region mutation on channel inhibition by tertiapin. (A−D) Current traces of the wild-type and three mutant channels, N124A, G127S, and F146A, recorded in the absence and presence of tertiapin at the concentrations indicated. (E) Fractions of unblocked current (I/I_o) for the wild-type and the three mutant channels were plotted as a function of the concentration of tertiapin. All data were corrected for the background leak current that was determined using high concentrations of tertiapin. The curves superimposed on the data correspond to the best least-squares fits using the equation $I/I_o = K_i/(K_i + [Tx])$, where [Tx] is toxin concentration. The determined inhibition constants were 2.0 ± 0.1, 13.9 ± 0.4, 2.7 ± 0.3, and 65.2 ± 4.0 nM (mean ± sem, $n = 4-16$) for the wild-type, N124A, G127S, and F146A channels, respectively.

simultaneously replace each of the four equivalent residues by introducing a single mutation in the cDNA encoding ROMK1. Because of this technical advantage, we chose to carry out a mutagenesis study in the ROMK1 channel.

We first examined how mutations in the P-region of the ROMK1 channel affect the interaction of the channel with tertiapin. Figure 5A−D shows the inhibition of the wild-type channel and three representative mutant channels (N124A, G127S, and F146A) by tertiapin. The affinity of the G127S channel for tertiapin was similar to that of the wild-type channel, whereas the affinities of N124A and F146A channels were much reduced. Fractions of unblocked currents for all four channels were plotted as a function of the concentration of tertiapin in Figure 5E. The equilibrium dissociation constants for the wild-type, N124A, G127S, and F146A channels were 2.0 nM, 13.9 nM, 2.7 nM, and 65.2 nM, respectively. Effects of 12 P-region mutations on the interaction of the channel with tertiapin were summarized in Figure 6.

For a comparison, we also examined tertiapin inhibition of a mutant channel in which asparagine 171, in the second putative membrane-spanning segment (M2), was replaced with an aspartate. The substitution of a negatively charged residue, aspartate, in the M2 segment is known to dramati-

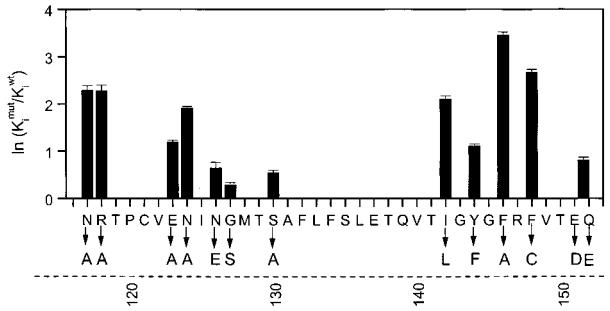

FIGURE 6: Summary of P-region mutation on the interaction of tertiapin with the ROMK1 channel. The free energy changes (in RT units) resulting from various P-region mutations were plotted against the primary sequence.

cally increase the channel affinity for intracellular cationic blockers such as Mg^{2+} and polyamines (*6*−*8*, *32*, *33*). As a consequence, the N171D channel conducts much smaller outward K^+ current than the wild-type channel (*6*, *32*, *33*; and also see Figure 7A,B). Despite the dramatic effect of the N171D mutation on the binding of the intracellular cations to the channel, the mutation had little effect on the binding of extracellular tertiapin (Figure 7A,B). The equilibrium dissociation constants of the wild-type and the mutant channels were 2.0 nM and 1.5 nM, respectively (Figure 7C). The data presented thus far are compatible with the idea that tertiapin inhibits the channel by binding to the P-region.

DISCUSSION

We have purified and identified a small protein in the honey bee venom, called tertiapin, as an inhibitor against two members of the inward-rectifier K^+ channel family. Both the GIRK1/4 and ROMK1 inward-rectifier K^+ channels are highly sensitive to tertiapin while the IRK1 inward-rectifier K^+ channel is relatively insensitive. Tertiapin was initially purified from the bee venom over 20 years ago (*28*). Because the venom was believed to contain materials beneficial to arthritis, many laboratories tried to identify the antiarthritis components in the venom. The search led to the purification of many small proteins. Two of the purified small proteins, apamin and MCDP, were found to be

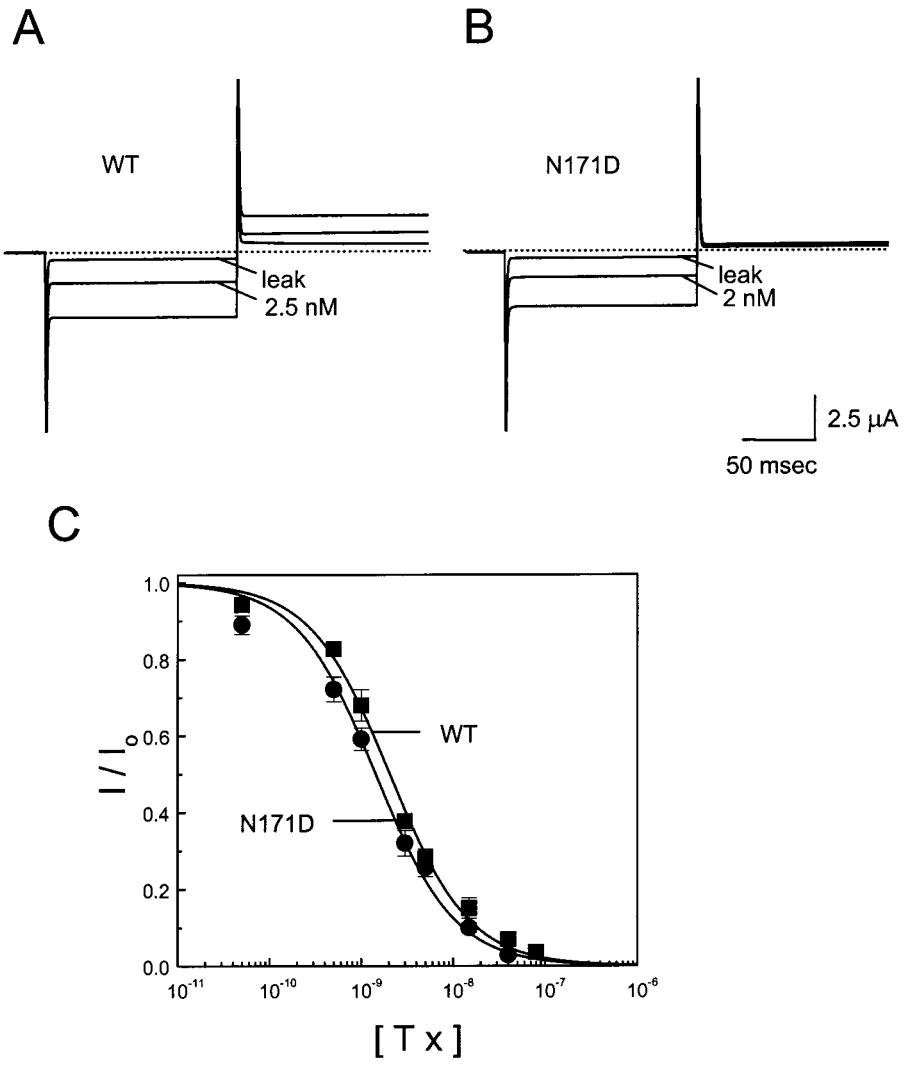

FIGURE 7: Effect of a ROMK1 M2-region mutation on channel inhibition by tertiapin. (A and B) Current traces of the wild-type (A) and N171D mutant (B) ROMK1 channels recorded in the absence and presence of tertiapin at the concentrations indicated. The dotted lines identify the zero current level. (C) Fractions of unblocked current (I/I_o) for both channels were plotted as a function of the concentration of tertiapin. All data were corrected for the background leak current determined using high concentrations of tertiapin. The curves superimposed on the data correspond to the best least-squares fits using the equation $I/I_o = K_i/(K_i + [Tx])$, where [Tx] is toxin concentration. The determined inhibition constants were 2.0 ± 0.1 and 1.5 ± 0.1 nM (mean ± sem; $n = 16-20$) for the wild-type and N171D mutant channels, respectively.

inhibitors of voltage- and Ca^{2+}-activated K^+ channels (*30*, *31*). Tertiapin is one of the many other purified proteins without any clearly identified biological activities.

Even though the biological action of tertiapin was unknown, the studies on tertiapin chemistry were quite advanced. The three-dimensional structure of tertiapin has been determined using NMR spectroscopy (*34*). The structure shows that tertiapin is a highly compact molecule with a high density of positively charged residues. It consists of a type-I reverse turn and an α-helix. A loop formed by an extended *β*-sheet connects the turn and the helix. Four cysteines within the polypeptide chain form two disulfide bonds. The extensive interactions among the side chains enhance the rigidity the structure of tertiapin. The overall structure of tertiapin is very similar to that of apamin (*35*). The main difference between these two structures is the relative position of the connecting loop and the α-helix. This difference is caused by the existence of an extra amino acid residue in the connecting loop of tertiapin. At this point, we do not know whether the difference in the relative position of the connecting loop and the α-helix, or the differences in the side chains of various residues, accounts for the greater than 100-fold difference in the affinities between the two toxins (Figures 2 and 3).

It has been well established that scorpion toxins inhibit the voltage- and Ca^{2+}-activated K^+ channels by blocking the ion conduction pore (*36*−*38*). Extensive mutagenesis studies have revealed much of the molecular interactions between the toxins and the channels (*39*−*49*). Recent crystallographic studies on a bacterial K^+ channel showed how the P-region makes up the outer part of the pore (*24*). The signature sequence forms the K^+-selective pore, and the residues C-terminal to the signature sequence form the base of the external vestibule, whereas the sequence N-terminal to the P-region constructs four turrets that surround the pore. When a scorpion toxin blocks the channel, it lies between two diagonally located turrets. The middle portion of the toxin contacts the vestibule base while the two ends contact the turrets (*50*). Because the channel is 4-fold symmetric, a toxin molecular can bind to the channel in four equivalent orientations.

In the present study, we found that mutations at the residues that form the turrets (e.g., N124) and the vestibule base (e.g., F146 and F148) affected tertiapin binding to the ROMK1 inward-rectifier K^+ channel. (The mutations around a glycosylation site, N117, in the P-region also affected tertiapin binding.) Furthermore, the ROMK1 P-region mutations that weaken the binding of tertiapin were known to weaken the binding of a scorpion toxin, Lq2 (*25*). These findings argue that a similar structure underlies both the scorpion toxin and the bee toxin receptors, re-enforcing the concept that all K^+ channels have a similar K^+-selective pore despite a lack of conservation at most P-region residues (except the signature sequence) among various classes of K^+ channels (*25*, *50*).

Contrary to what has been found for Lq2, a channel mutation, I142L, lowers the affinity of the ROMK1 channel for tertiapin by 8-fold. Residue 142 is located within the signature sequence that forms the K^+-selective part of the pore (*23*, *24*). The different effects of the mutation I142L on the binding of the two toxins may be a consequence that tertiapin contacts the base of the vestibule more intimately than Lq2, which would also explain why tertiapin binds to the channel with a 200-fold higher affinity than Lq2 does (*25*, Figure 2).

Tertiapin is an asymmetric molecule, while the ROMK1 channel is likely 4-fold symmetric because it is formed by four identical subunits (*9*). The ROMK1 channel should have four identical binding orientations for tertiapin, similar to those for scorpion toxins on the voltage-activated K^+ channels. However, the GIRK1/4 inward-rectifier K^+ channel is formed by two different types of subunits (GIRK1 and GIRK4) with a 2:2 stoichiometry (*51*−*53*). The GIRK1/4 channel likely does not contain four equivalent binding orientations for tertiapin. Therefore, an understanding of how tertiapin interacts with GIRK1/4 channel may provide insight into the arrangement of the subunits, i.e., whether the same two subunits are located adjacently or diagonally.

In summary, we report here a nanomolar affinity inhibitor, tertiapin, for two inward-rectifier K^+ channels, GIRK1/CIR and ROMK1. Tertiapin will be a very useful tool for studying the physiology and the structure−function relationship of these channels. Tertiapin will also be a powerful ligand for purifying functional channels as well as for screening pharmaceutical agents against these channels.

ACKNOWLEDGMENT

We thank L. Y. Jan for GIRK1 and IRK1 clones, D. E. Clapham for CIR clone, K. Ho and S. Hebert for ROMK1 clone, and E. G. Peralta for HM2 and HM4 clones. We also thank C. Deutsch, R. MacKinnon, J. Rush, and K. J. Swartz for helpful discussion and/or for critical reading of our manuscript. Amino acid analysis, mass spectrometry, protein sequencing, and peptide synthesis were performed by the Bioploymer Facility, Harvard Medical School.

REFERENCES

1. Katz, B. (1949) *Arch. Sci. Physiol. 2*, 285−299.
2. Hille, B. (1991) *Ionic channels of excitable membranes*, Sinauer Associates, Inc., Sunderland, MA.
3. Matsuda, H., Saigusa, A., and Irisawa, H. (1987) *Nature 325*, 156−159.
4. Vandenberg, C. A. (1987) *Proc. Natl. Acad. Sci. U.S.A. 84*, 2560−2564.
5. Horie, M., Irisawa, H., and Noma, A. (1987) *J. Physiol. 387*, 251−272.
6. Lopatin, A. N., Makhaina, E. N., and Nichols, C. G. (1994) *Nature 372*, 366−369.
7. Ficker, E., Taglialatela, M., Wible, B. A., Henley, C. M., and Brown, A. M. (1994) *Science 266*, 1068−1072.
8. Fakler, B., Branle, U., Glowatzki, E., Weidemann, S., Zenner, H. P., and Ruppersberg, J. P. (1995) *Cell 80*, 149−154.
9. Ho, K., Nichols, C. G., Lederer, W. J., Lytton, J., Vassilev, P. M., Kanazirska, M. V., and Hebert, S. C. (1993) *Nature 362*, 127−132.
10. Kubo, Y., Baldwin, T. J., Jan, Y. N., and Jan, L. Y. (1993) *Nature 362*, 127−132.
11. Kubo, Y., Reuveny, E., Slesinger, P. A., Jan, Y. N., and Jan, L. Y. (1993) *Nature 364*, 802−806.
12. Dascal, N., Schreibmayer, W., Lim, N. F., Wang, W., Chavkin, C., DiMagno, L., Labarca, C., Kieffer, B. L., Gaveriaux-Ruff, C., Trollinger, D., Lester, H., and Davidson, N. (1993) *Proc. Natl. Acad. Sci. U.S.A. 90*, 10235−10239.
13. Krapivinsky, G., Gordon, E. A., Wickman, K., Velimirovic, B., Kraplvinsky, L., and Clapham, D. E. (1995) *Nature 374*, 135−141.

14. Inagaki, N., Gonoi, T., Clement, J. P., IV, Namba, N., Inazawa, J., Gonzalez, G., Aguilar-Bryan, L., Seino, S., and Bryan, J. (1995) *Science 270*, 1166−1170.
15. Pfaffinger, P. J., Martin, J. M., Hunter, D. D., Nathanson, N. M., and Hille, B. (1985) *Nature 317*, 536−538.
16. Breitweitser, G. E., and Szabo, G. (1985) *Nature 317*, 538−540.
17. Logotheis, D. E., Kurachi, Y., Galper, J., Neer, E. J., and Clapham, D. E. (1987) *Nature 325*, 321−326.
18. Wickman, K. D., Iniguez-Lluhi, J. A., Davenport, P. A., Taussing, R., Krapivinsky, G. B., Linder, M. E., Gilman, A. G., and Clapham, D. E. (1994) *Nature 368*, 255−257.
19. Reuveny, E., Slesinger, P. A., Inglese, J., Morales, J. M., Iniguez-Lluhi, J. A., Lefkowitz, R. J., Bourne, H. R., Jan, Y. N., and Jan, L. Y. (1994) *Nature 370*, 143−146.
20. Fakler, B., Brandle, U., Glowatzki, E., Zenner, H.-P., Zenner, and Ruppersburg, J. P. (1994) *Neuron 13*, 1413−1420.
21. Huang, C.-L., Feng, S., and Hilgemann, D. W. (1988) *Nature 391*, 803−806.
22. Heginbotham, L., Abramson, T., and MacKinnon, R. (1992) *Science 258*, 942−944.
23. Heginbotham, L., Lu, Z., Abramson, T., and MacKinnon, R. (1994) *Biophys. J. 66*, 1061−1067.
24. Doyle, D., Cabral, J. M., Pfuetzner, R. A., Kuo, A., Gulbis, J. M., Cohen, S. L., Chait, B. T., and MacKinnon, R. (1998) *Science 280*, 69−77.
25. Lu, Z., and MacKinnon, R. (1997) *Biochemistry 36*, 6936−6940.
26. Lucchesi, K., Ravindran, A., Young, H., and Moczydlowski, E. (1989) *J. Membr. Biol. 109*, 269−281.
27. Escobar, L., Root, M., and MacKinnon, R. (1993) *Biochemistry 32*, 6982−6987.
28. Gauldie, J., Hanson, J. M., Rumjanek, F. D., Shipolini, R. A., and Vernon, C. A. (1976) *Eur. Biochem. 61*, 369−376.
29. Ovchinnikov, Y. A., Miroshnikov, A. I., Kudelin, A. B., Kostina, M. B., Boikov, V. A., Magzanik, L. G., and Gotgilf, I. M. (1980) *Bioorg. Khim. 6*, 359−365.
30. Blatz, A. L., and Magleby, K. L. (1986) *Nature 323*, 718−720.
31. Stuhmer, W., Ruppersburg, J. P., Schroter, K. H., Sakmann, B., Stocker, M., Giese, K. P., Perschke, A., Baumann, A., and Pongs, O. (1989) *EMBO J. 8*, 3235−3244.
32. Lu, Z., and MacKinnon, R. (1994) *Nature 371*, 243−246.
33. Wible, B. A., Taglialatela, M., Ficker, E., and Brown, A. M. (1994) *Nature 371*, 246−249.
34. Xu, X., and Nelson, J. W. (1993) *Protein: Struct., Funct., Genet. 17*, 124−137.
35. Pease, J. H., and Wemmer, D. E. (1988) *Biochemistry 27*, 8491−8498.
36. MacKinnon, R., and Miller, C. (1988) *J. Gen. Physiol. 91*, 335−349.
37. Miller, C. (1988) *Neuron 1*, 1003−1006.
38. Park, C.-S., and Miller, C. (1992) *Neuron 9*, 307−313.
39. MacKinnon, R., and Miller, C. (1989) *Science 245*, 1382−1385.
40. MacKinnon, R., Heginbotham, L., and Abramson, T. (1990) *Neuron 5*, 767−771.
41. Stampe, P., Kolmakova-Partensky, L., and Miller, C. (1994) *Biochemistry 33*, 443−450.
42. Goldstein, S. A. N., Pheasant, D. J., and Miller, C. (1994) *Neuron 12*, 1377−1388.
43. Stocker, M., and Miller, C. (1994) *Proc. Natl. Acad. Sci. U.S.A. 91*, 9509−9513.
44. Gross, A., Abramson, T., and MacKinnon, R. (1994) *Neuron 13*, 961−966.
45. Hidalgo, P., and MacKinnon, R. (1995) *Scinece 268*, 307−310.
46. Aiyar, J., Withka, J. M., Rizzi, J. P., Singleton, D. H., Andrews, G. C., Lin, W., Boyd, J., Hansoon, D. C., Simon, M., Dethlets, B., Lee, C. L., Hall, J. E., Gutman, G. A., and Chandy, K. G. (1995) *Neuron 15*, 1169−1181.
47. Rangananthan, R., Lewis, J. H., and MacKinnon, R. (1996) *Neuron 16*, 131−139.
48. Naranjo, D., and Miller, C. (1996) *Neuron 16*, 123−130.
49. Gross, A., and MacKinnnon, R. (1996) *Neuron 16*, 399−406.
50. MacKinnon, R., Cohen, S. L., Kuo, A., Lee, A., and Chait, B. T. (1998) *Science 280*, 106−109.
51. Silverman, S. K., Lester, H. A., and Dougherty, D. A. (1996) *J. Biol. Chem. 271*, 30524−30528.
52. Tucker, S. J., Pessia, M., and Adelman, J. P. (1996) *Am. J. Physiol. 271*, H379−H385.
53. Corey, S., Krapivinski, G., Krapivinsky, L., and Clapham, D. E. (1998) *J. Biol. Chem. 273*, 5271−5278.

BI981178P